CALCIUM PHOSPHATE THIN FILMS DEPOSITED AT GLANCING ANGLE BY RADIOFREQUENCY MAGNETRON SPUTTERING UNDER CONSTANT SUBSTRATE ROTATION

K. A. Prosolov, O. A. Belyavskaya, V.V. Lastovka, O. Prymak, J. Rau, M. Epple, Yu. P. Sharkeev

Institute of Strength Physics and Materials Science of SB RAS, Tomsk, Russia

National Research Tomsk Polytechnic University, Russia

Istituto di Struttura della Materia, Consiglio Nazionale delle Ricerche (ISM-CNR), Rome, Italy

Inorganic Chemistry and Center for Nanointegration Duisburg-Essen (CeNIDE), University of Duisburg-Essen

Tomsk – 2020

Challenges of orthopedic surgeries

COMPLICATIONS in prosthetics (%)

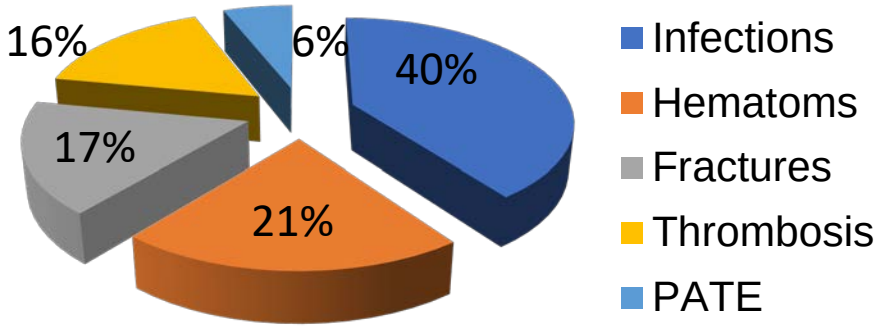

REASONS for revision prosthetics (%)

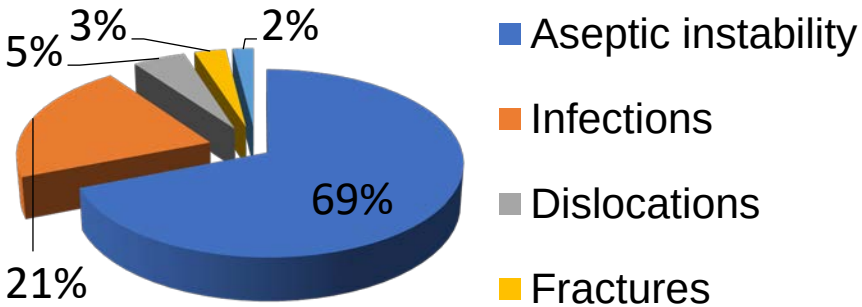

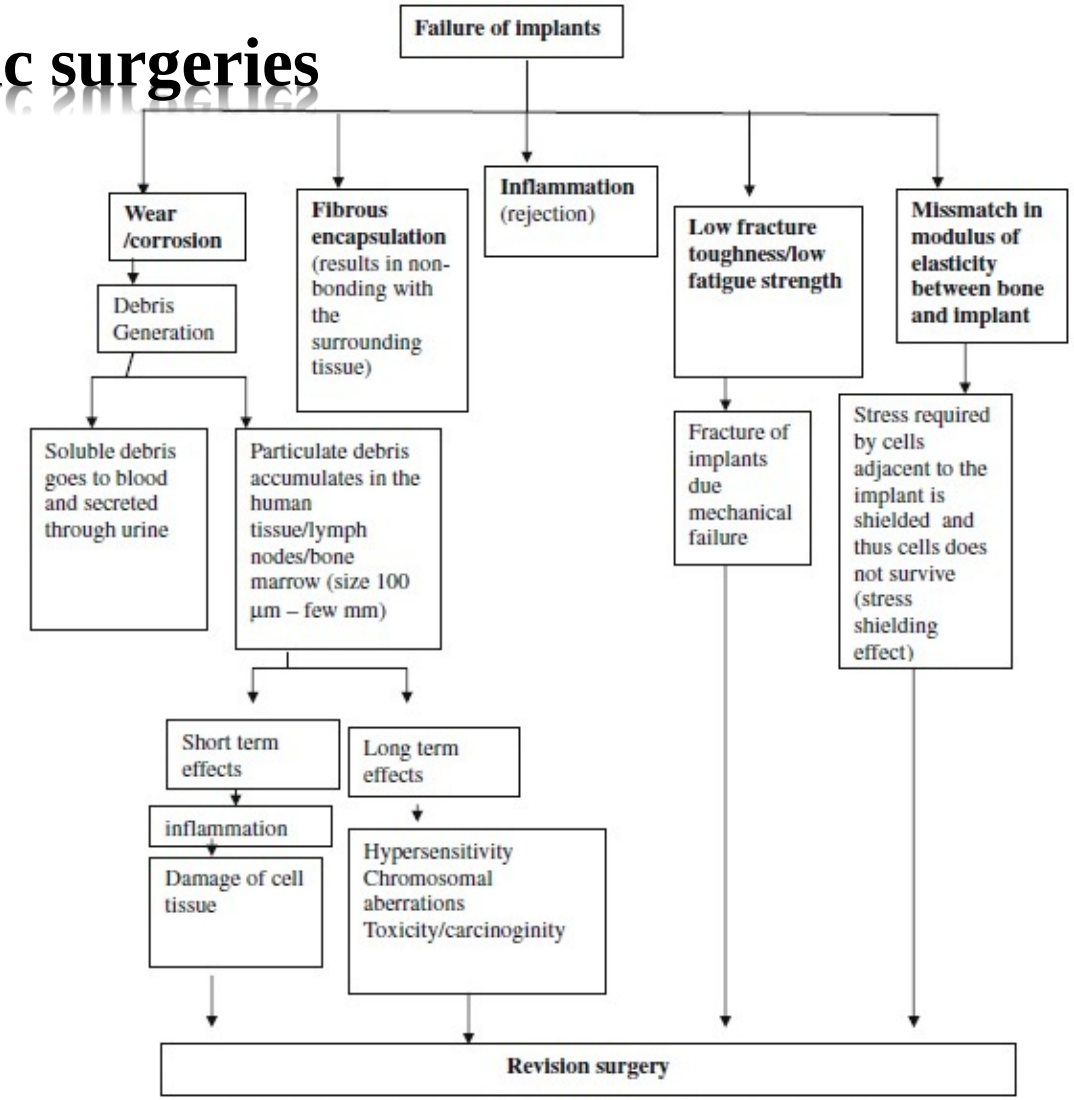

- Development of implant materials based on metallic substrate and calcium phosphate coating that should be viable when in contact with living tissue to perform their function, their chemical composition, structure and physical and mechanical properties should be close to those of bone tissue.

N.V. Zagorodny, Scientific-practical conference "Vreden reading" (2013)

Geetha M., Singh A.K., Asokamani R., Gogia A.K. Prog. Mat. Sci. 2009;54: P. 397–425.

Cell Response and Surface Topography

- It has been shown that the creation of nanopatterns is a powerful tool for directing stem cell fate.
- Given that different cell types show different responses to different surface topographies, there is continuous need for the development of “next generation” biomaterials and medical implants. The surface properties of biomaterials, that is, porosity or wettability are important for their application and critical for the adhesion process of adjacent cells in the case of implants.

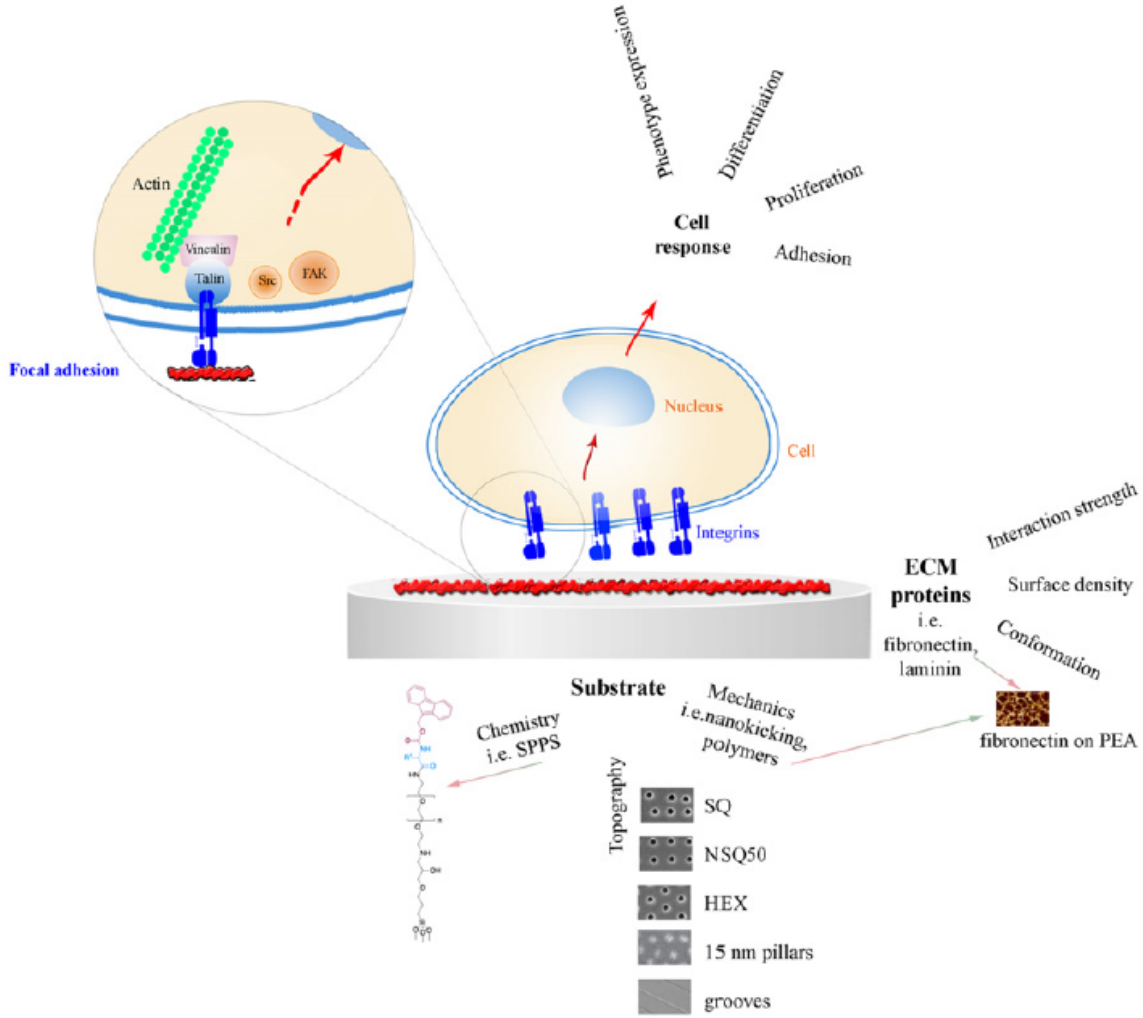

Fig. 1 Schematic diagram of cell mechanical stimulation through cell/protein/material interactions. Cells are exposed to different types of forces: extracellular such as tensile/traction forces through the ECM interacting with surface proteins that control cell adhesion and intracellular cytoskeletally generated contractile forces such as actomyosin contraction. Material properties such as chemistry, topography, mechanical properties, influence cell response to the density and strength of interaction between the material surface and the adsorbed ECM proteins. Receptor activation through integrin binding to RGD sequence on the ECM proteins, leads to initiation of signaling cascades, and hence changes in gene expression and consequently modulation of protein expression and cellular functions such as survival, proliferation and differentiation. DOI:10.1016/B978-0-12-803581-8.10226-7

Surface Topography and Antibacterial Effect

Another advantage is that high aspect ratio nanopatterns are capable of killing bacteria and preventing biofilm formation.

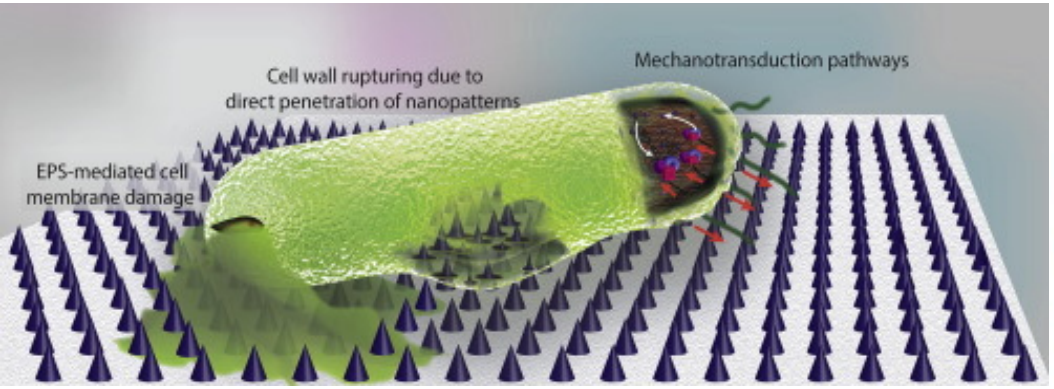

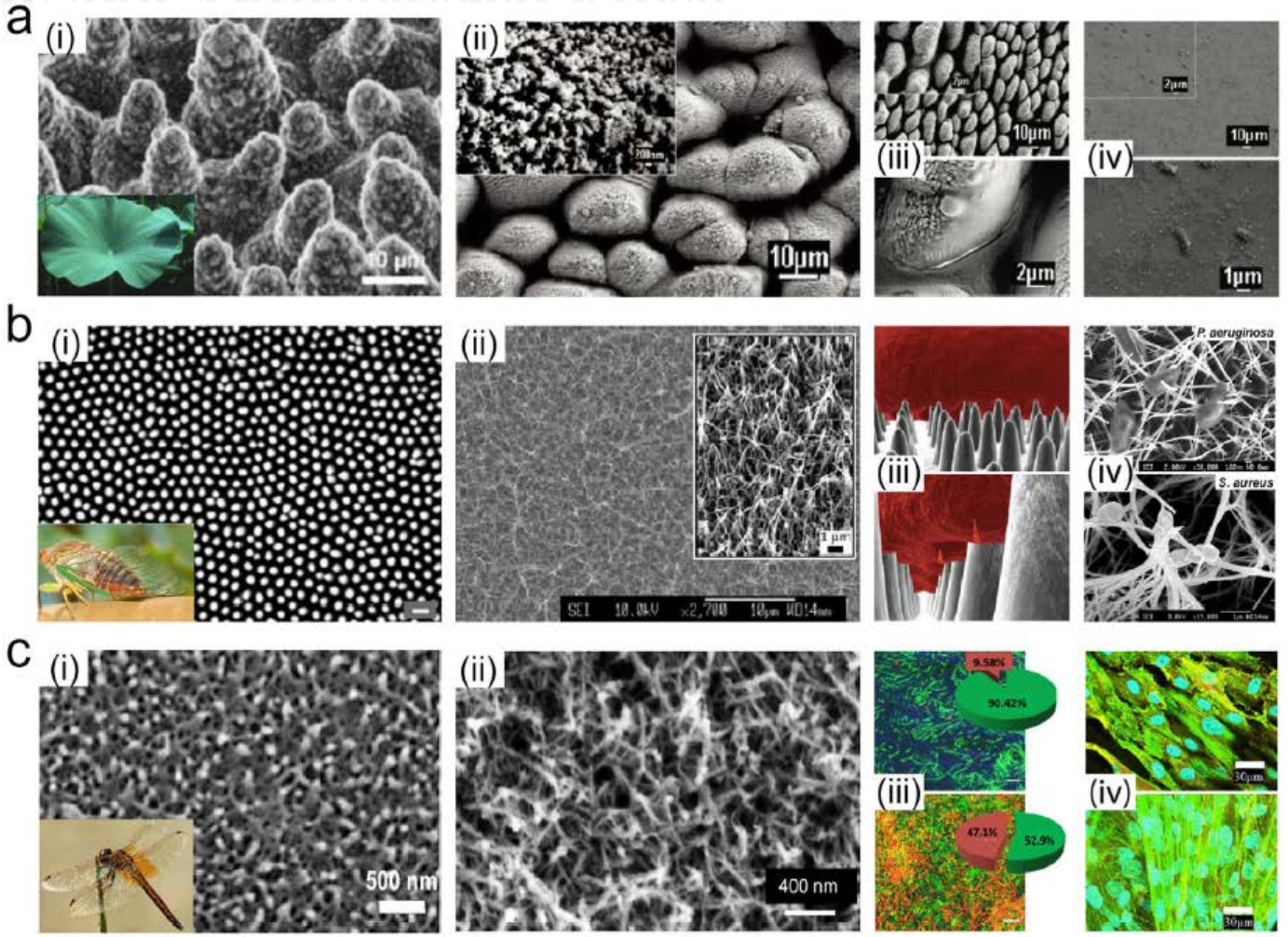

Fig. 9. (a) (i) Optical and SEM images of the lotus leaf (upper side) (Ensikat et al., 2011). (ii) SEM images of femtosecond laser ablated Ti surface inspired by lotus leaf. SEM images of *P. aeruginosa* attachment patterns taken at different magnifications on the (iii) structured and (iv) polished Ti surfaces after 18 h incubation (Fadeeva et al., 2011). (b) (i) Optical and SEM images of cicada wing surface. (ii) SEM images of alkaline hydrothermally treated Ti surface with TiO_2 nanowire arrays inspired by Cicada wing surface, the inset is a 30° tilted view showing sharp nanowire tips; (iii) Three-dimensional representation of the cellular attachment and rupture on the cicada wing surface nanopillars; (iv) SEM images of nanowire-pierced bacterial cells after one-hour incubations on bioinspired titania surface under dynamic conditions (Pogodin et al., 2013; Diu et al., 2014). (c) (i) Optical and SEM images of the dragonfly wing surface (Gao et al., 2013). (ii) SEM images of hydrothermal etching Ti surface with TiO_2 nanopatterned arrays inspired by dragonfly wing surface; (iii) Confocal scanning laser microscope (CSLM) images of *P.aeruginosa* attachment on the (top) untreated and (bottom) nanopatterned Ti surfaces reveal the viable (stained green with SYTO 9) and the non-viable cells (stained red with Propidium Iodide) (Scale Bar: 10 μm). The antibacterial activity of both substrates was shown in the individual pie charts. (iv) Adhesion and proliferation of human primary fibroblasts on the (top) untreated and (bottom) nanopatterned Ti surfaces after incubation periods of 10 days (Bhadra et al., 2015).

DOI: 10.1016/j.actbio.2018.09.059

DOI: 10.1039/C7BM01016H

Methods for Manufacturing of Patterned Surfaces

- There are many approaches that could help to manufacture an artificial patterned surfaces. Methods such as:

- **photolithography;**
- **laser holography;**
- **colloidal lithography;**
- **mask anodization;**
- **surface chemistry methods**, etc. are successfully employed for this purpose.

- However, abovementioned methods usually require sophisticated equipment and frequently are time consuming.

- **Is there a way to deposit patterned surfaces by using PVD technique only?**

Glancing Angle Deposition

- During conventional film deposition, a stream of vapour-phase atoms strikes and condenses upon a perpendicular substrate to form a dense, solid film.
- In Glancing angle deposition (GLAD) the substrate is tilted to a glancing angle, thus creating an oblique deposition geometry. As the atoms condense on the substrate they spontaneously form microscopic nuclei. Ballistic (i.e. line-of-sight) shadowing prevents incoming vapour from condensing into regions behind the nuclei, causing the nuclei to develop into columns that tilt towards the vapour source. The shadowing mechanism in an oblique deposition geometry causes the condensing vapour to self-assemble into oriented columnar nanostructures.

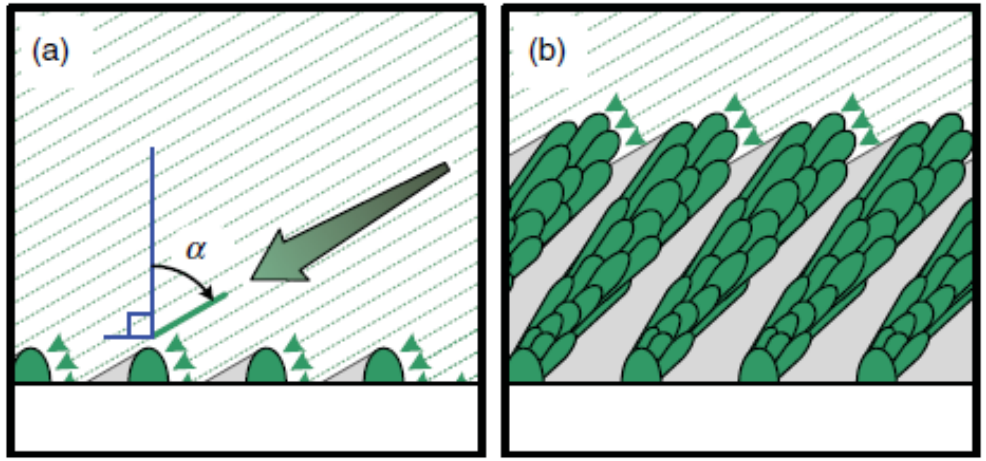

A conceptual view of the GLAD process. (a) The incident vapour atoms, arriving at an angle α with respect to the surface normal, are intercepted by the growing nanocolumns. (b) Shadowed regions are thus created where no growth occurs, and vapour deposition is restricted to the nanocolumns that grow towards the vapour source.

Glancing Angle Deposition: Properties and Examples

- The fabrication of columnar films with controlled porosity is a central feature of obliquely deposited films.
- By using GLAD to engineer the nanoscale structure, film properties can be controlled and tuned over a substantially greater range than typically achieved with conventional film deposition.
- Consider that by using GLAD, any compatible material can be transformed into a highly porous film exhibiting greatly enhanced surface area and a tailored mesopore structure.

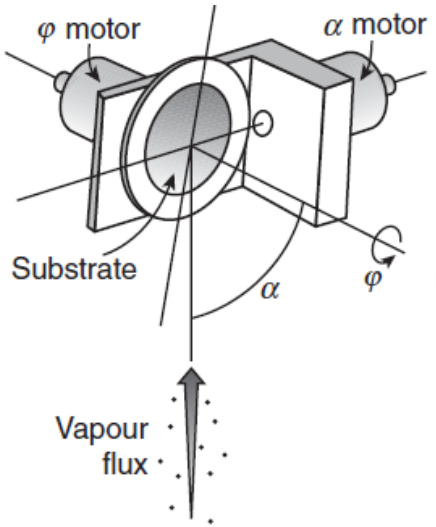

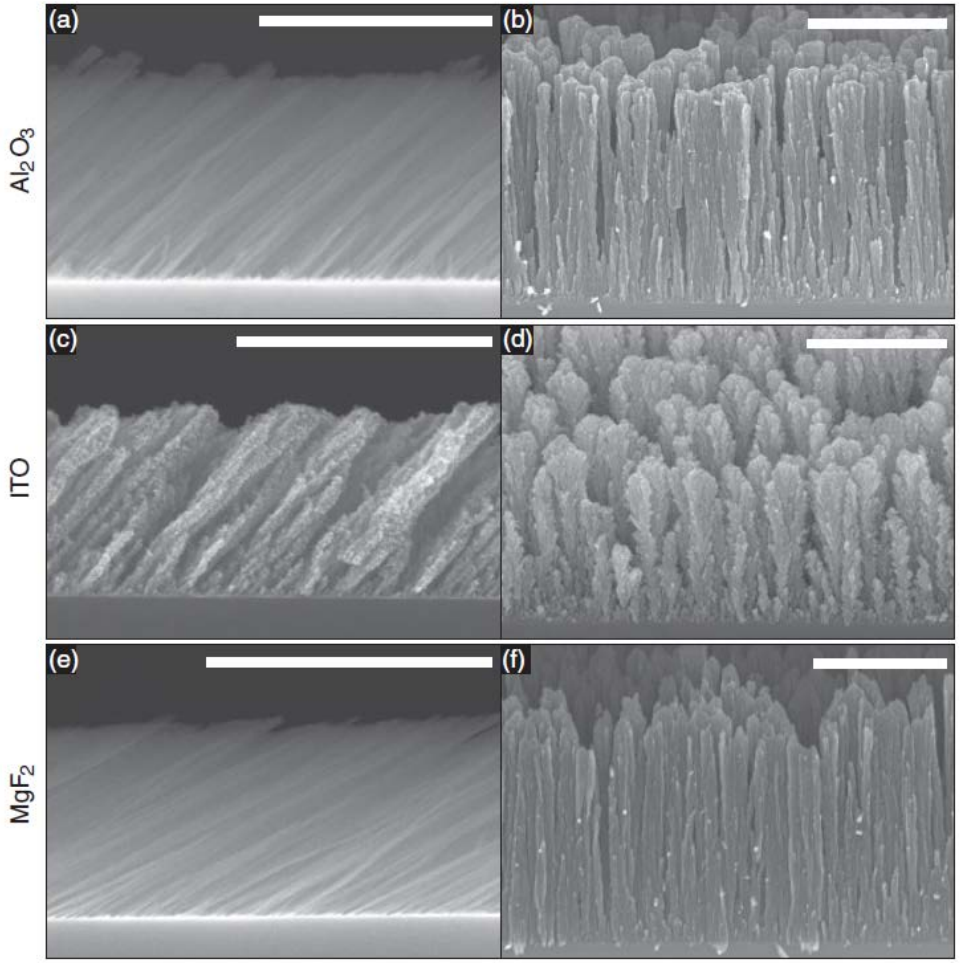

Tilted columnar films of (a, b) Al2O3, (c, d) ITO, and (e, f) MgF2, each deposited at α = 85◦ and without substrate rotation. To a first-order approximation, the films all possess the same general tilted columnar morphology, as the ballistic deposition process underlying GLAD is similar for each material*.

*Sorge, J.B. (2012) Argon-assisted glancing angle deposition, PhD thesis, University of Alberta

GLAD: Broad Material Compatibility

Because GLAD is based upon physical vapour deposition techniques it inherits much of the broad material compatibility provided by PVD thin-film deposition. This flexibility is a major scientific and technological advantage as GLAD can therefore be used to fabricate diverse nanostructural morphologies in materials with a wide range of physicochemical properties.

However, GLAD of complex compounds such as hydroxyapatite or other calcium phosphates has not been yet reported in the literature.

Material	PVD method	Ref.	Material	PVD method	Ref.
Elements			HfO_2	E-beam	[1]
Ag	E-beam	[2,3]	InN	IP	[4]
Al	Thermal, e-beam	[5,6]	In_2S_3	Thermal	[7]
Au	Sputtering	[8]	ITO	E-beam	[9–11]
C	IBS, PLD, E-beam	[12–14]	MgF_2	Thermal	[15,16]
Cr	E-beam, sputtering	[17,18]	MgO	Effusion	[19]
Co	Thermal, e-beam	[20–22]	MoO_3	E-beam	[23]
Cu	E-beam, thermal, sputtering	[21,24,25]	Nb_2O_5	E-beam	[26,27]
Ge	E-beam	[28,29]	RuO_2	Sputtering	[8]
Fe	Thermal, MBE	[30–32]	SiO	Thermal	[17,33]
Mg	E-beam	[34,35]	SiO_2	E-beam	[10,16]
Mn	Evaporation	[36]	Ta_3N_5	Evaporation	[37]
Nb	Sputtering	[38,39]	Ta_2O_5	E-beam	[40–42]
Ni	E-beam	[43]	TiAlN	Sputtering	[44]
Pd	Effusion	[45]	TiC	E-beam	[46,47]
Pt	E-beam, sputtering	[48–50]	TiO_2	E-beam	[51–53]
Ru	Sputtering	[50,54]	TiZrV	Sputtering	[55]
Se	Thermal	[56]	WO_3	Sputtering, thermal	[57–59]
Si	E-beam	[60,61]	$W_xSi_yO_z$	Sputtering	[59,62]
Ta	E-beam, sputtering	[63,64]	Y_2O_3:Eu	E-beam	[65,66]
Te	Thermal	[56]	YSZ	E-beam	[67,68]
Ti	Sputtering, e-beam	[69–71]	ZnO	PLD, e-beam, sputtering	[72,73]
W	Sputtering	[21,58,74]	ZnS	E-beam	[75]
Inorganic			ZrO_2	E-beam	[41,76]
Al_2O_3	E-beam	[77,78]			
As_2O_3	Thermal	[79,80]	*Organic*		
ATO	E-beam	[81]	Alq_3	Thermal	[82,83]
$BiVO_4$	E-beam	[84]	C_{60}	Thermal	[85]
CaF_2	Thermal	[15,86]	CuPc	Thermal	[87]
CeO_2	E-beam	[88]	α-NPD	Thermal	[89]
CrN	Sputtering	[90]	Parylene C	Nozzle	[91]
Fe_2O_3	E-beam	[92]	Pentacene	Thermal	[85]
GeSbSn	Thermal	[93]	PPX	Nozzle	[94]
$GeSe_2$	Thermal	[95]			

The aim of the study - reproduce the physico-mechanical antibacterial effect of the nanocolumnar cicada wing surface for metallic biomaterials by fabrication of Ti nanocolumnar surfaces using GLAD. Nanocolumnar Ti thin films were fabricated by GLAD on silicon substrates. S. aureus as well as E. coli were incubated.

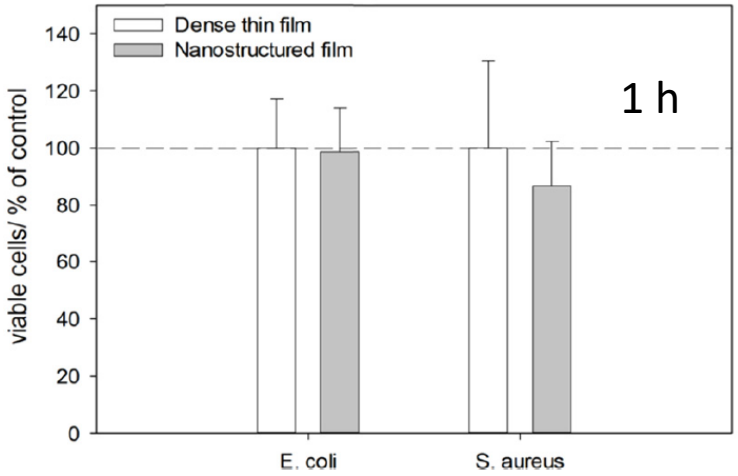

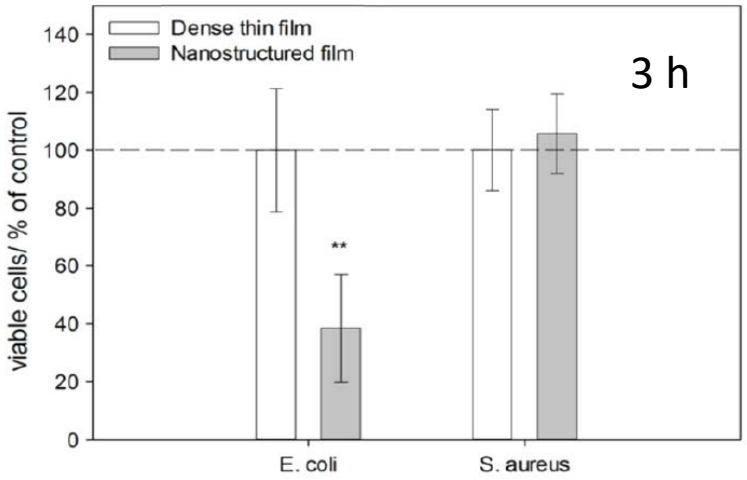

The viability of E. coli was significantly decreased after 3 h on the nanostructured film compared to the dense film and was accompanied by an irregular morphology and a cell wall deformation.

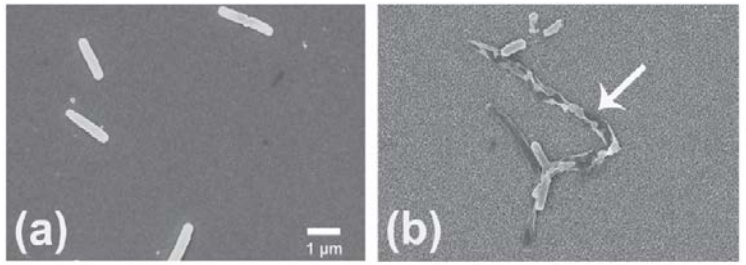

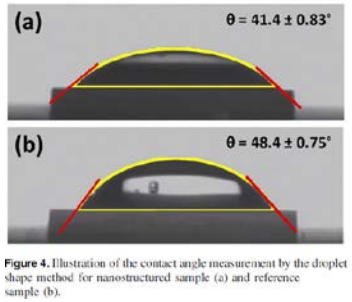

Figure 4. Illustration of the contact angle measurement by the droplet shape method for nanostructured sample (a) and reference sample (b).

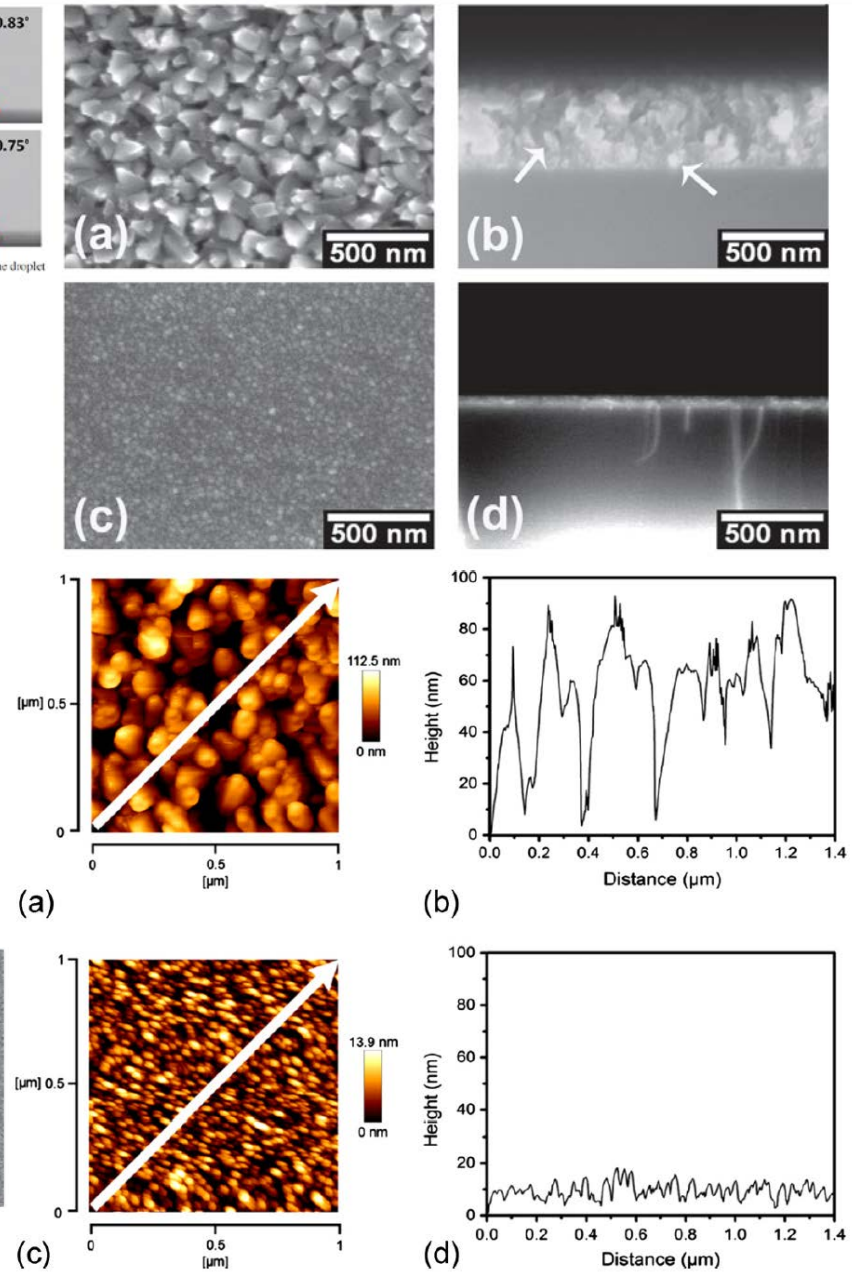

Figure 3. AFM topography images (a, c) and cross section profile along the white arrow (b, d) of the nanostructured and reference film, respectively.

* Sengstock C. et al. Structure-related antibacterial activity of a titanium nanostructured surface fabricated by glancing angle sputter deposition //Nanotechnology. – 2014. – Т. 25. – №. 19. – С. 195101.

Materials & Methods

A vacuum installation with an RF (13.56 MHz) magnetron source was used to deposit pure HA or TCP, HA-0.4Zn, HA-0.2Cu and biphasic HA/TCP coatings. The calcium phosphate powders are prepared by mechanochemical activation and then are used as a precursor-powder in order to prepare a target for sputtering.

In our research commercially pure titanium plates and polished Si wafers with the sizes of 10x10 mm^2 are usually used. CP Ti material is the main material of implants and surgical instruments in medicine.

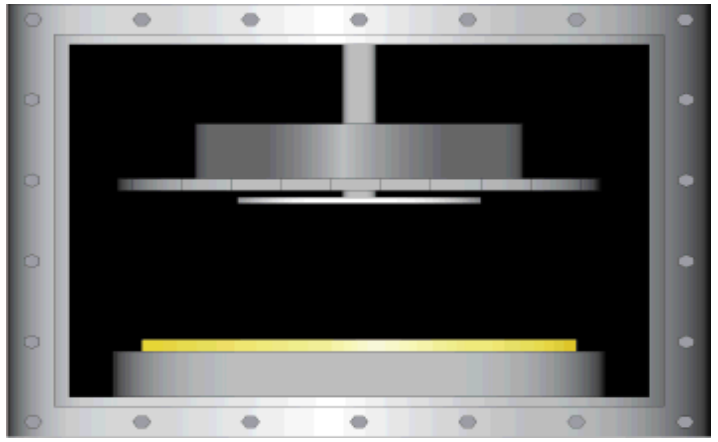

Vacuum installation equipped with the source of ions, magnetron system and rotating table with a heating plate.

Experimental Design and Deposition Parameters

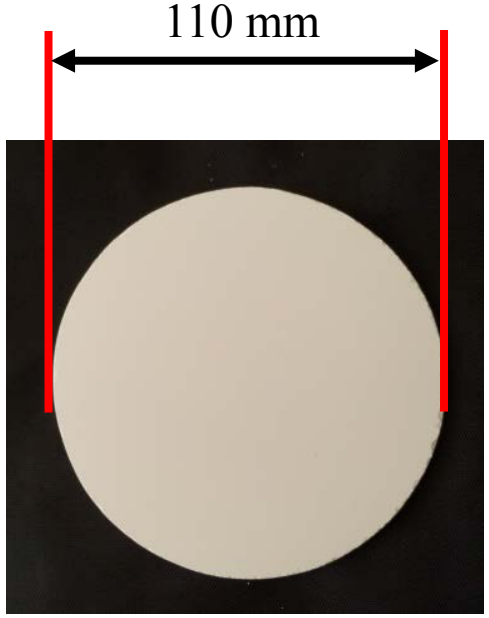

Sintered target of HA-0.4Zn is going to be bonded to the surface of the magnetron for sputtering.

The powder was pressed and then sintered in air at 1100 ºC for 1 h. The chemical composition of the powder and the target was confirmed by X-ray powder diffraction (XRD) and Fourier transform infrared spectroscopy (FTIR)

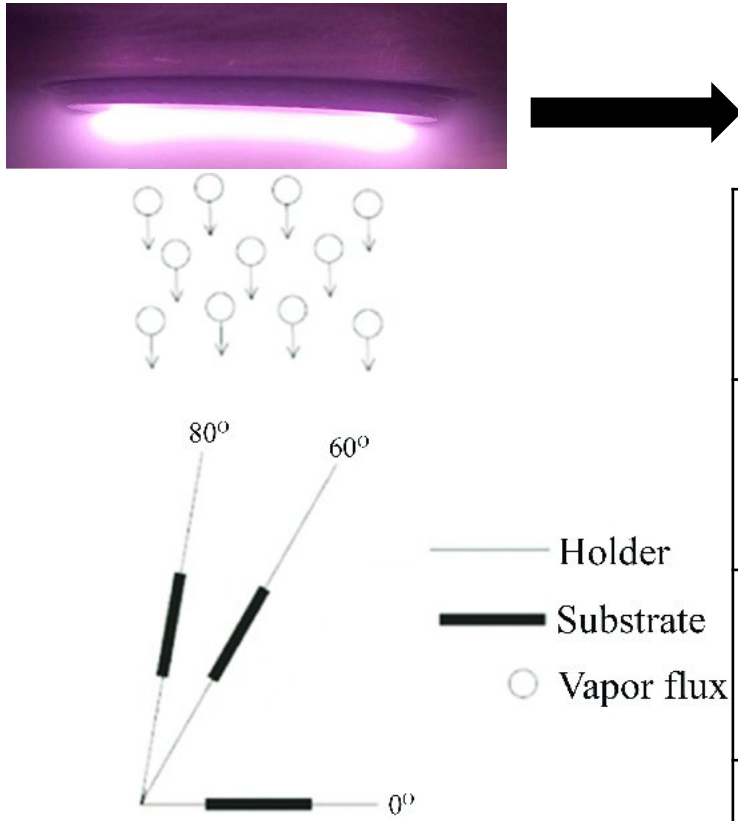

Schematic image of the deposition process of the Ti and Si samples with a variation in particle incidence angle of 0º, 60º and 80º during the RF magneton sputtering of a Zn-HA target.

Deposition Parameters

Deposition Angle,	Pressure, mTorr	Sputtering time, minutes	Target to Substrate distance, mm	Power, W	Power Density, W/cm^2	Substrate Material
0; 80	0,8	120	45	350	3,68	Si, Ti
0; 60; 80	0,8; 4,5	80; 120; 180	45	300	3,15	
0; 80	0,8	120; 180	45; 70	250	2,63	
0; 80	0,8	120	45	200	2,1	

Surface Morphology of the HA-Zn Coatings on Si

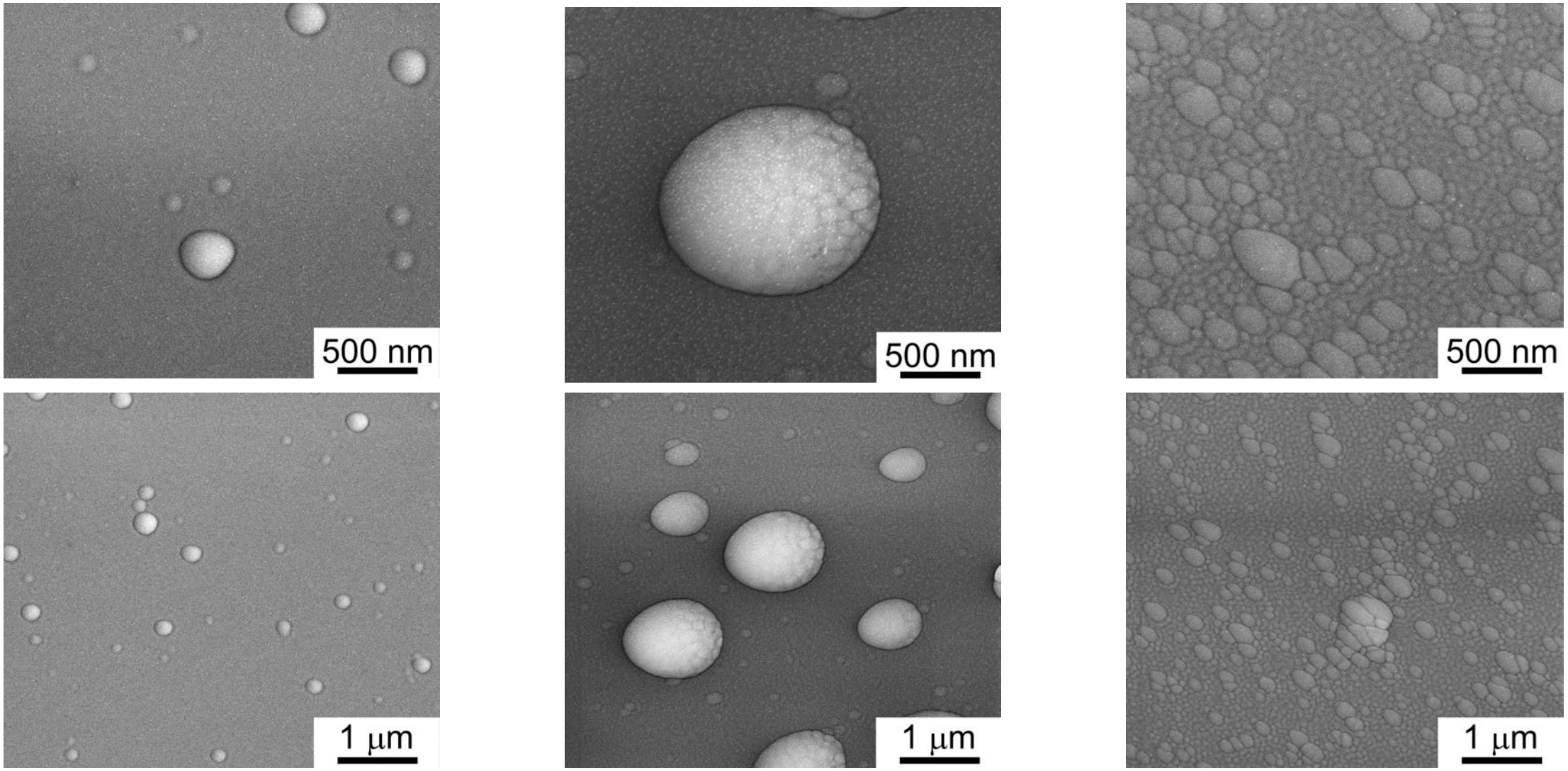

HA-Zn coatings deposited on Si at working gas pressure of 4.5 mTorr, Power Density 3,15 W/cm^2 under tilt angle of 0º (A), 60º (B), 80º (C) on Si substrates.

Cross-Section SEM Imaging

SEM cross-section images of obliquely deposited Zn-doped CaP thin films deposited on Si under tilt angles of 0° (a) and 80° (b) at 100,000× magnification and films under tilt angles of 0° (c) and 80° (d) at 200,000× magnification on Si substrates, demonstrating significant changes in the film morphology. The arrows indicate the angle of incidence θ. The columns are tilted by angle β.

EDX data obtained from both types of the samples showed that the Ca/P ratio equals to 1.8-1.9 while the content of Zn does not exceed 1 at%.

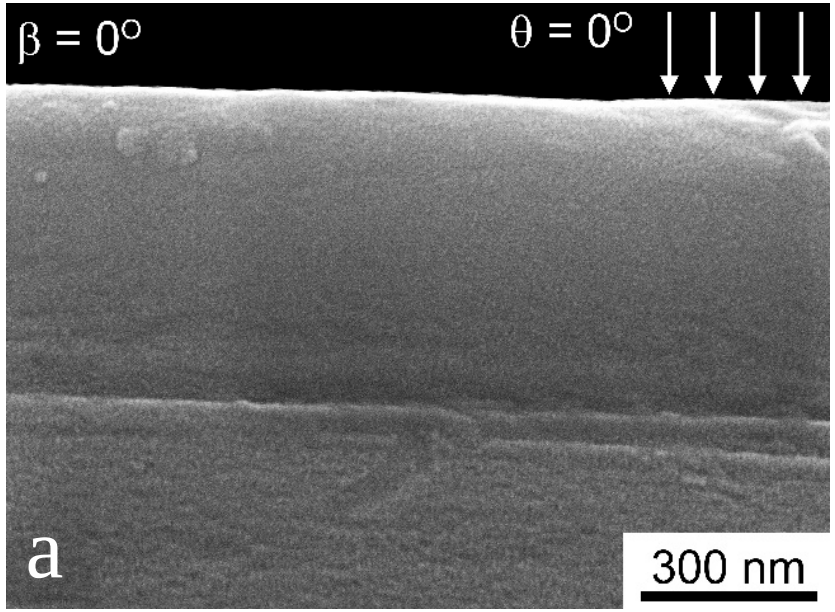

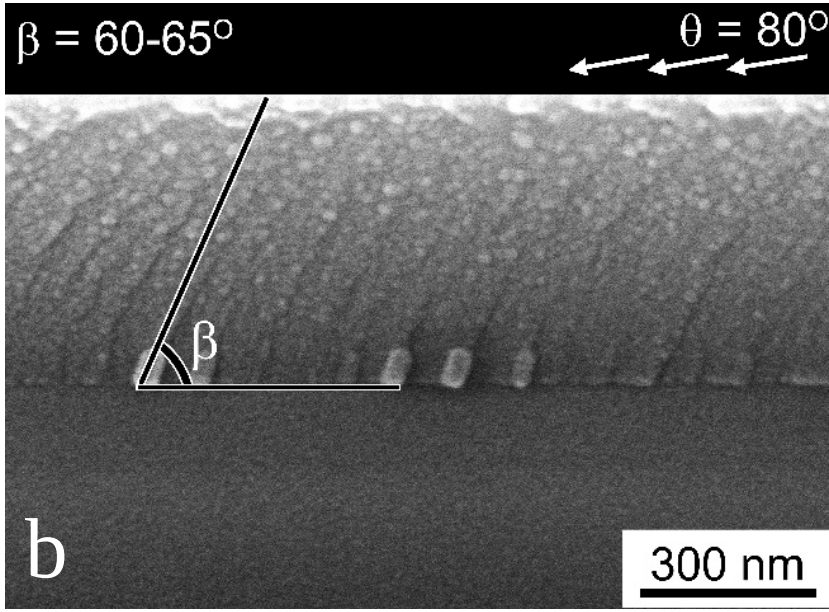

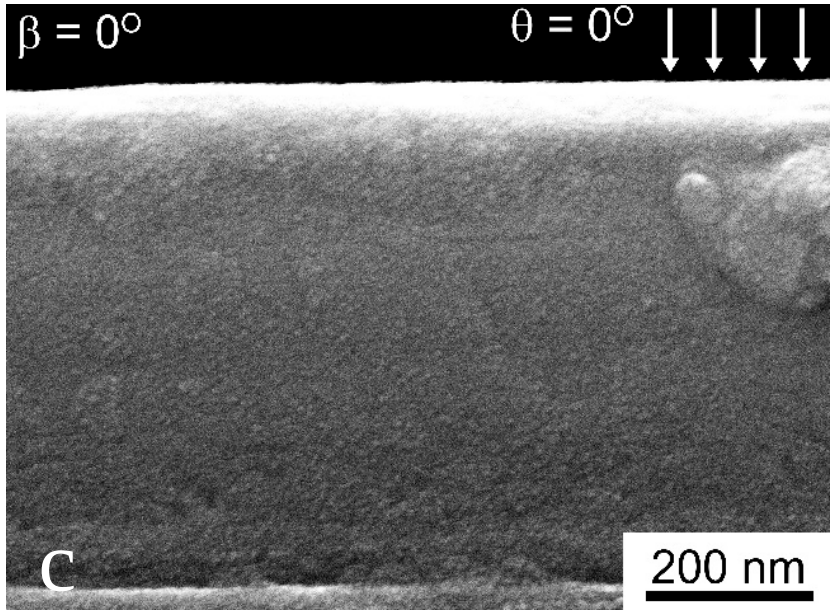

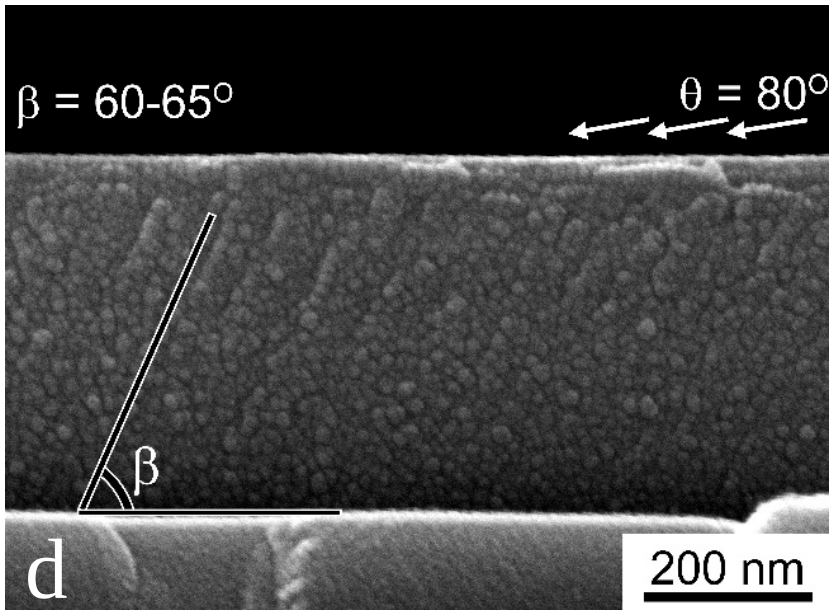

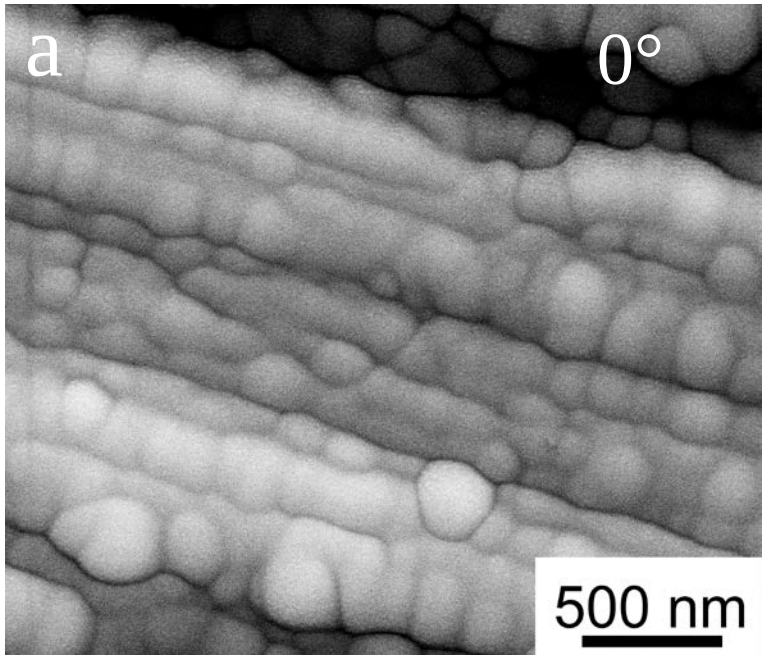

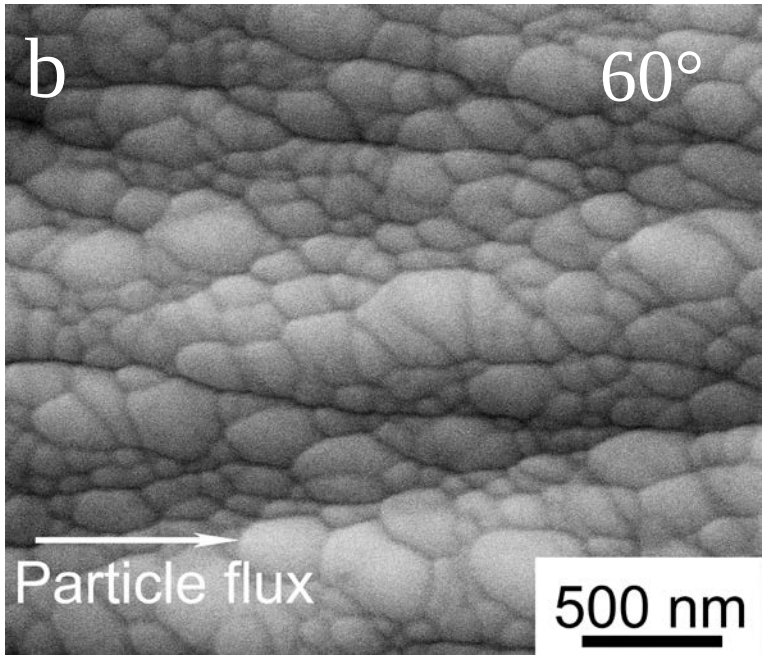

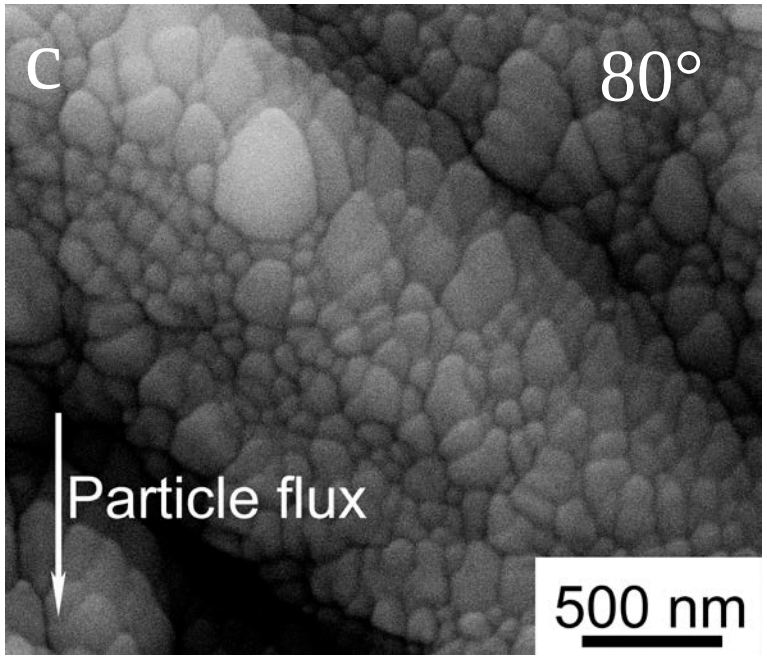

HA-Zn coatings deposited on Ti at a working gas pressure of 4.5 mTorr without tilting.

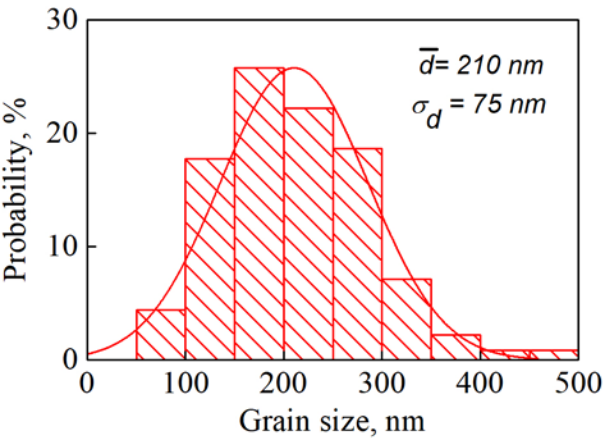

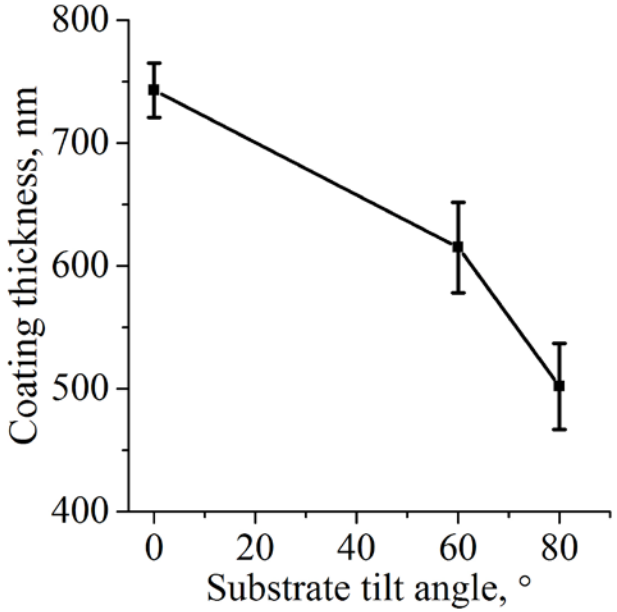

Plot of the coating thickness against the substrate tilt angle

HA-Zn coatings deposited on Ti at a working gas pressure of 4.5 mTorr under tilt angle of 80°.

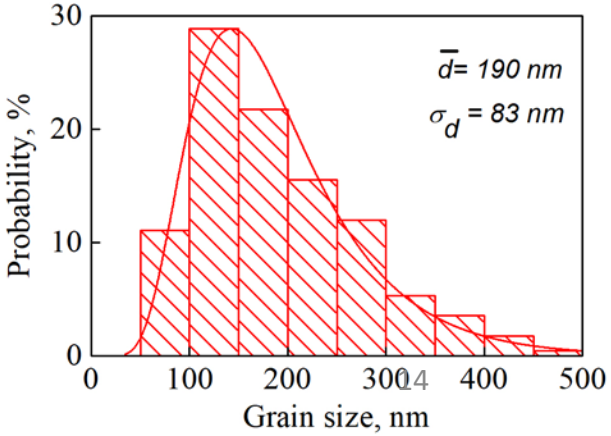

Atomic Force Microscopy of the Deposited HA-Zn Films

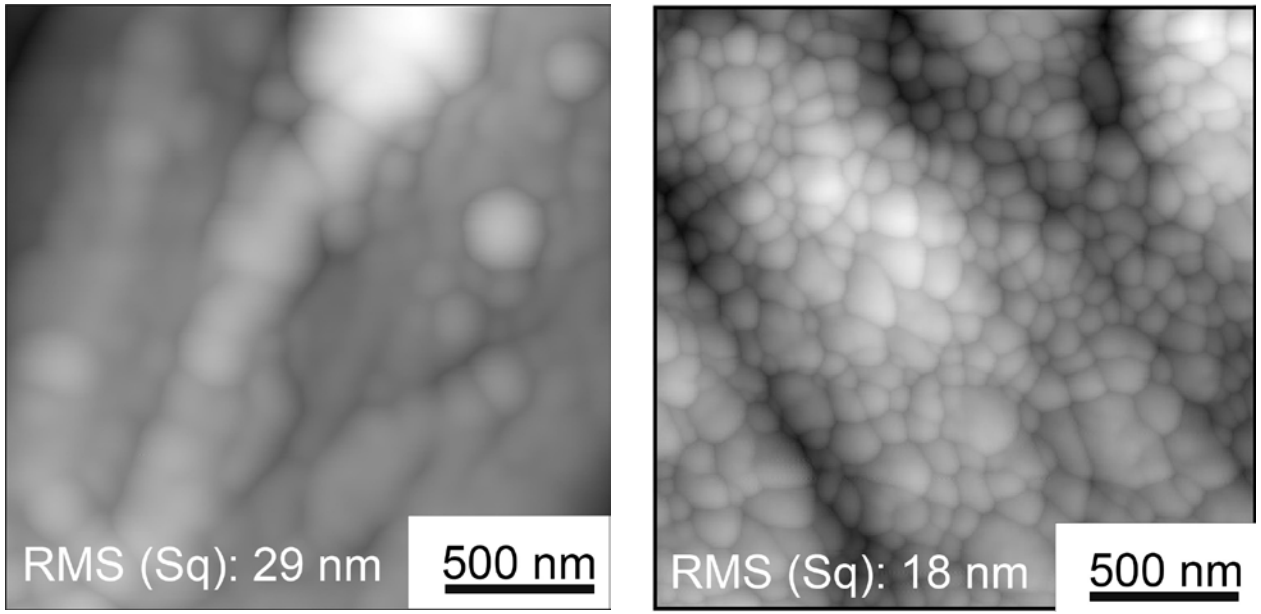

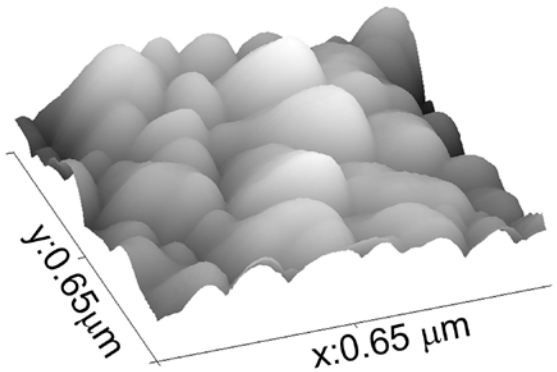

HA-Zn coatings deposited on Si at working gas pressure of 4.5 mTorr under inclination angle of 0º (a), 80º (b) and 3D visualization of coating deposited under 80º (c).

We believe that the difference in the RMS is due to the small sized surface grains which homogeneously cover the initial rough Ti surface are reducing the RMS compared to the sample without any inclination. In the case of the normal incidence of sputtered particles, globular shaped grains are formed on top of the Ti surface which increasing the RMS value.

Distribution of coting's surface features across the substrate

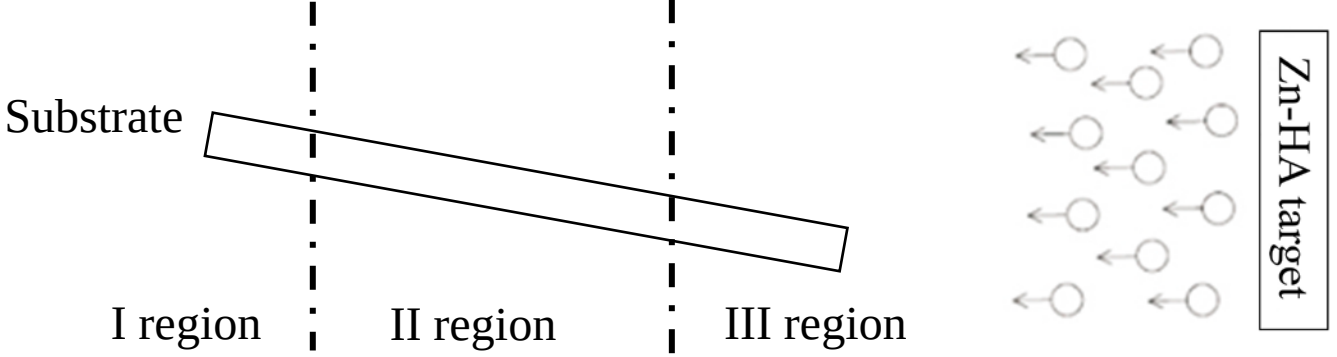

HA-Zn coatings deposited on Si substrate

HA-Zn coatings deposited on Ti substrate

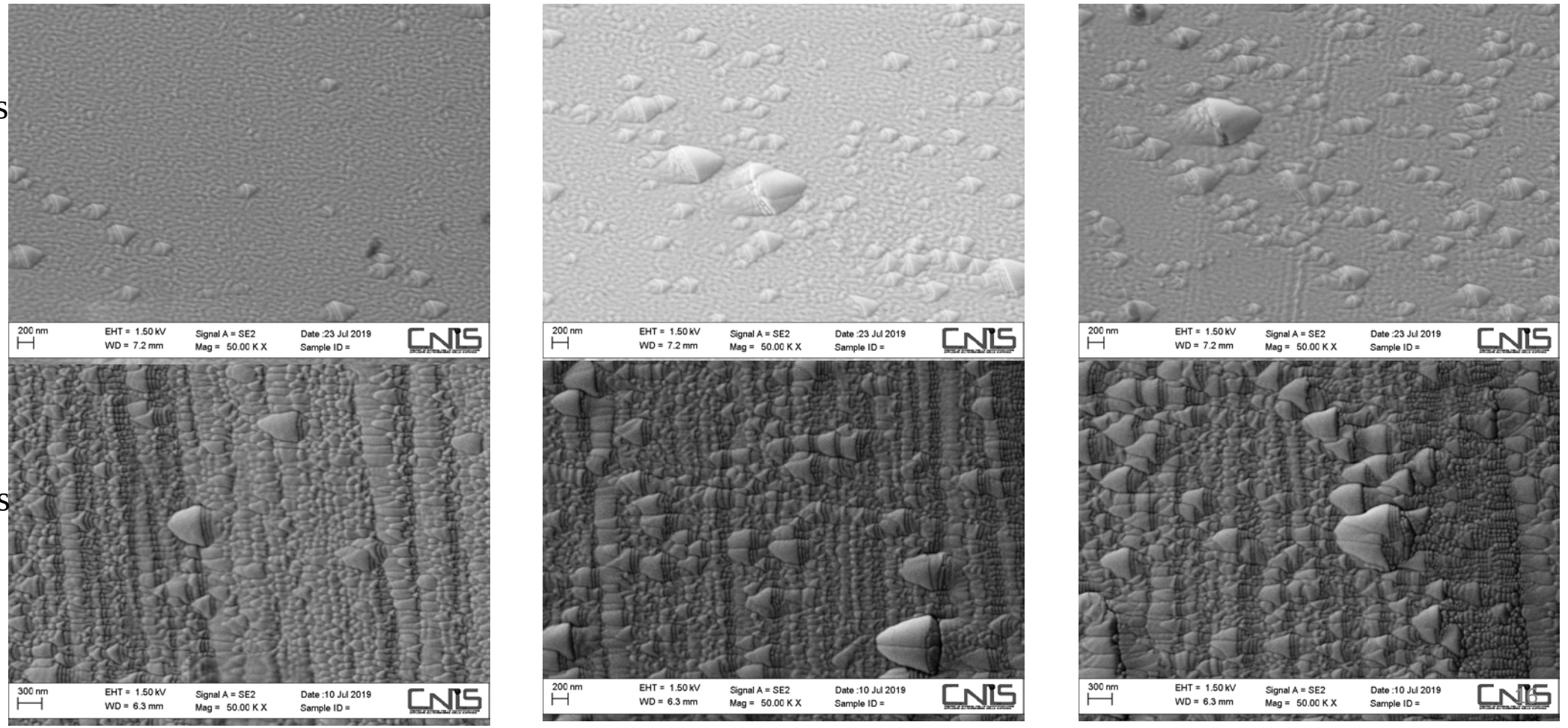

Distribution of surface features on the substrate

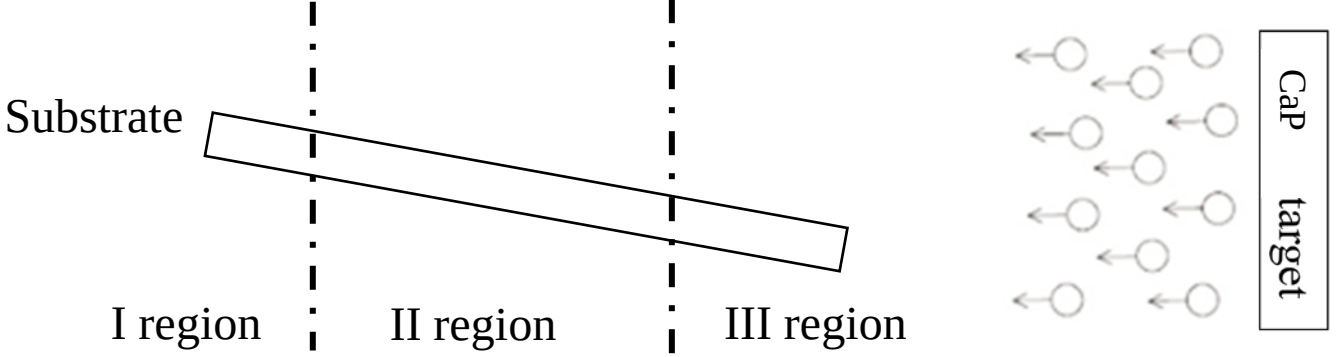

HA-Cu coatings deposited on Ti substrate

HA-Zn coatings deposited on Ti substrate

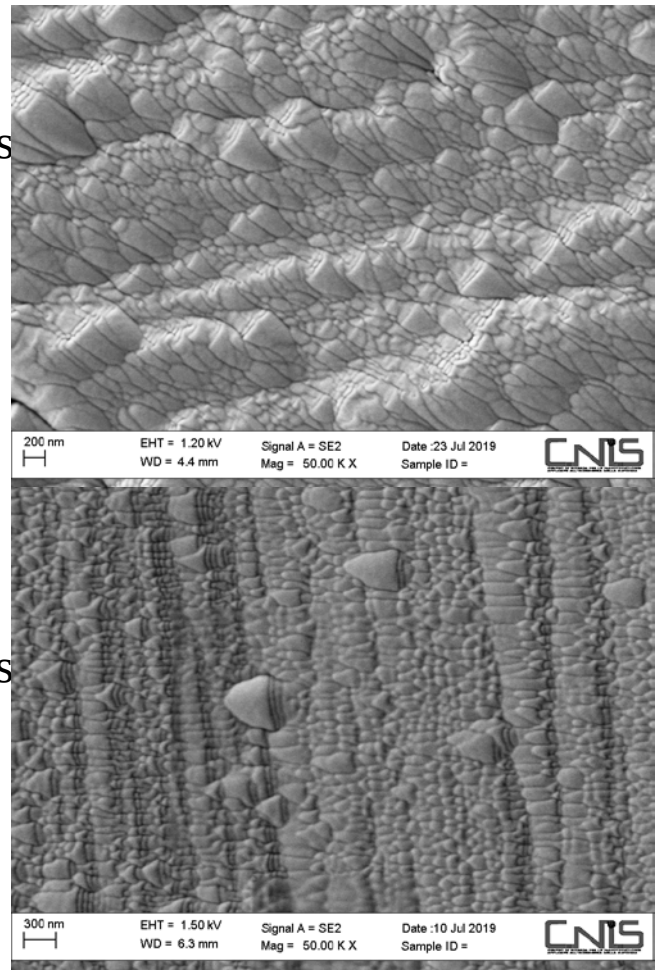

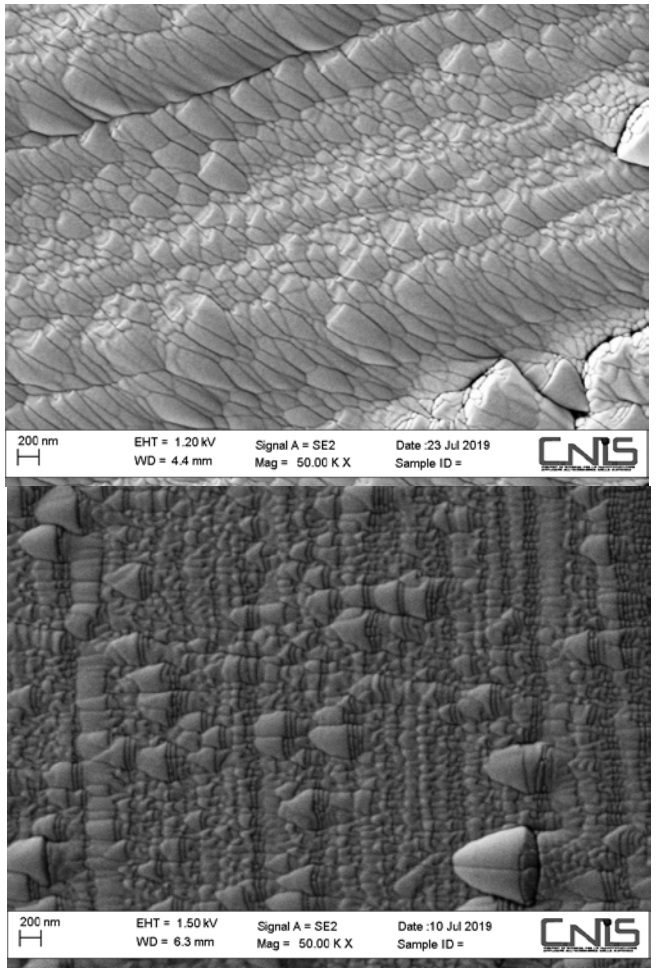

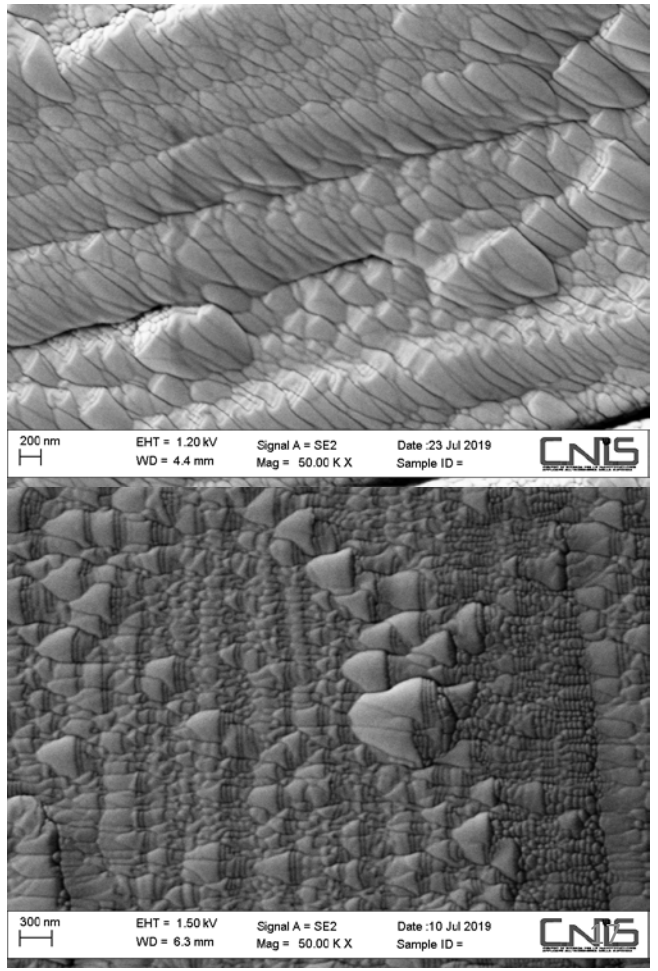

GLAD at Constant substrate rotation

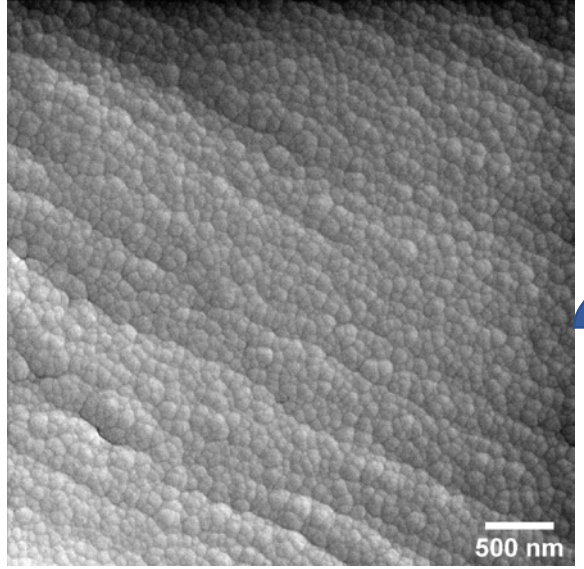

HA-Cu coatings deposited on Ti substrate.
Deposition at constant 5 RPM substrate rotation.

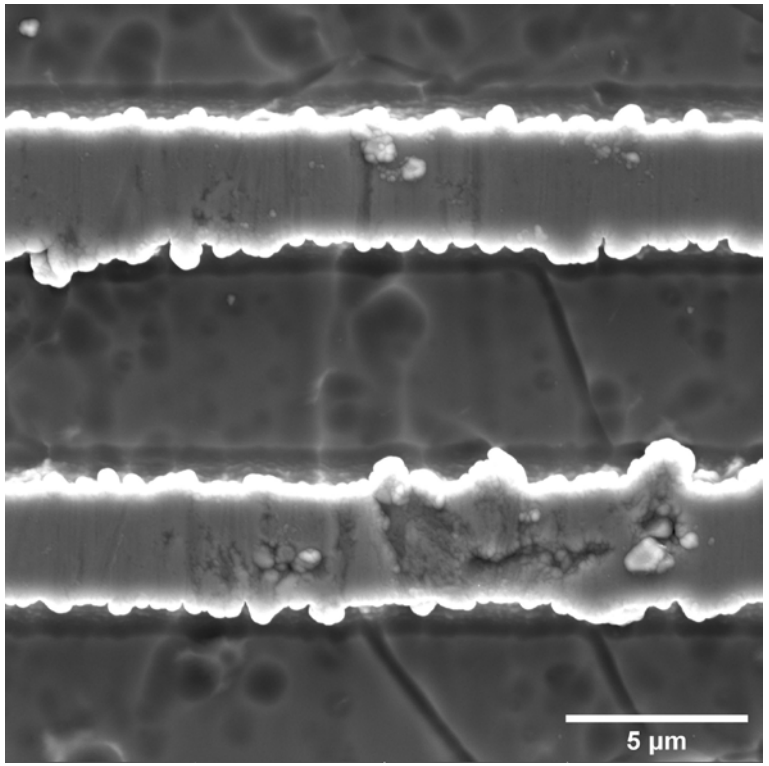

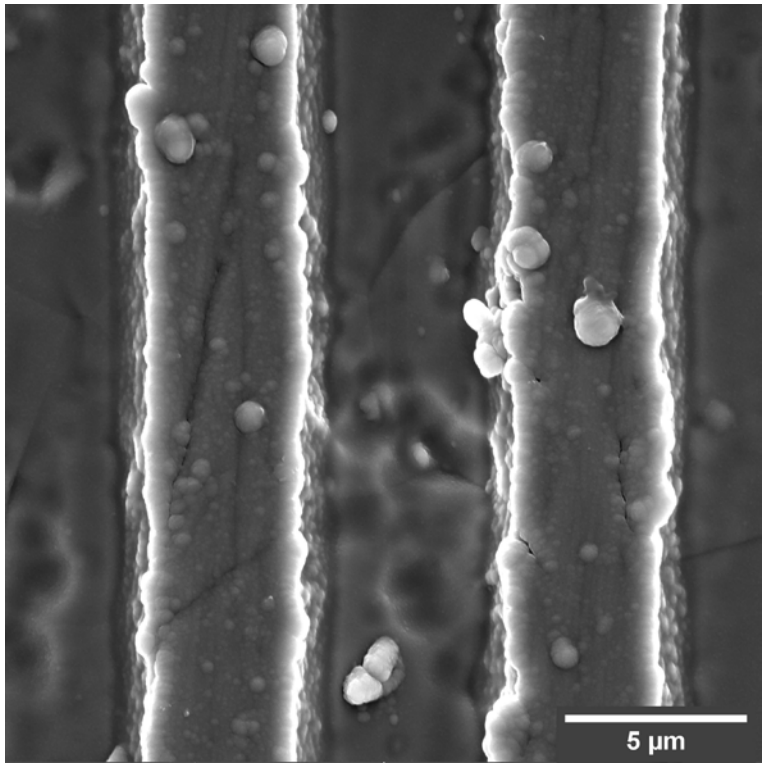

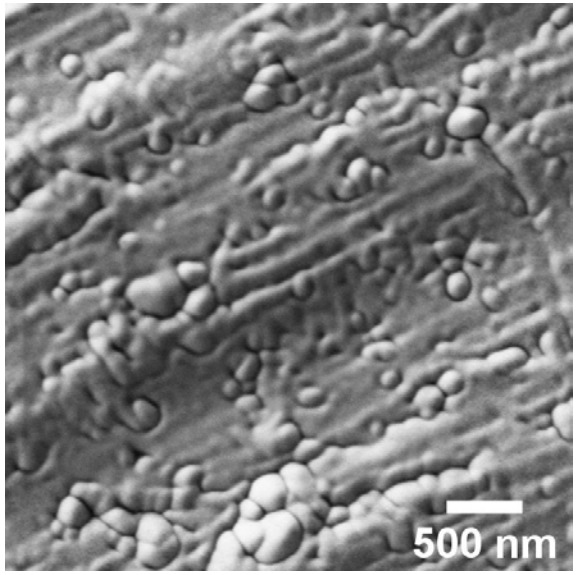

HA-Cu coatings deposited on Ti substrate.
Stationary normal flux deposition.

Conclusions and Future Perspectives

- It was shown that it is possible to manipulate the surface roughness and morphology of the coatings by variation of the substrate tilt angle.
- It was also shown that GLAD is a powerful technique that allows to vary CaP thin films morphology and can be utilized to create self-organized nanostructures that could be used for synergetic antibacterial effect.
- Improved collimation of the particle flux is needed for enhancement of self-shadowing.
- High precision motorized sample holder is needed for manufacturing more complex GLAD structures.
- Biological assessment is crucial for understanding the effect of GLAD morphology on cell response.

Questions?
I've got answers.

Thank you for your attention.
Please feel free to contact me as our lab is always open for collaboration!

Konstantin Prosolov,
Jr. Researcher at the Physics of nanostructured biocomposites laboratory of ISPMS SB RAS,
PhD student at Tomsk Polytechnic University.
Email: konstprosolov@gmail.com

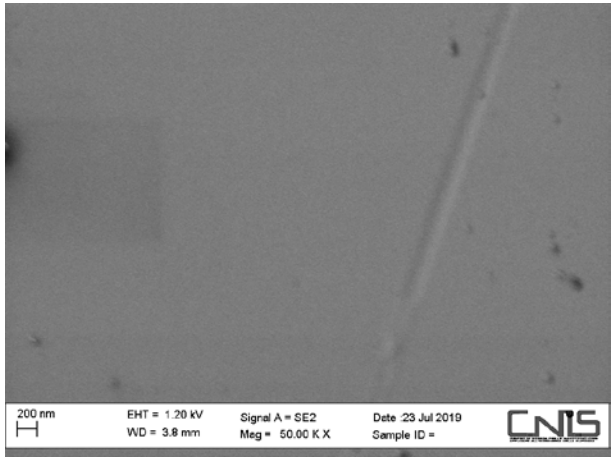

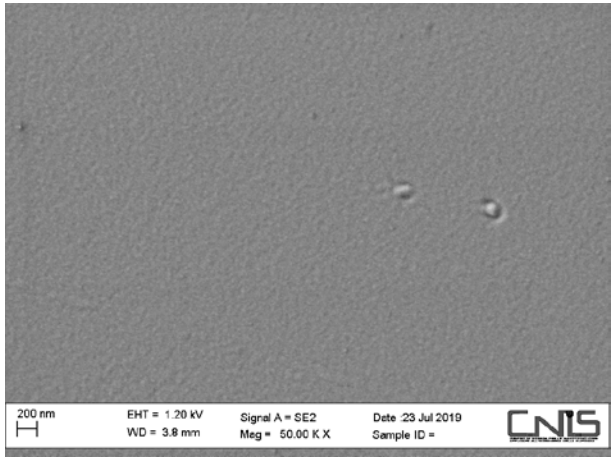

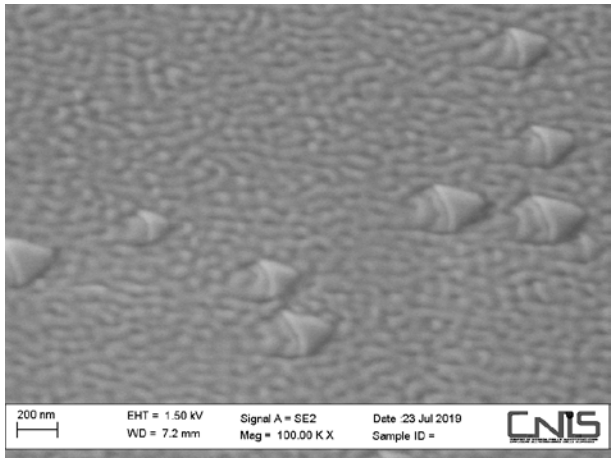

HA Zn 0 M_01

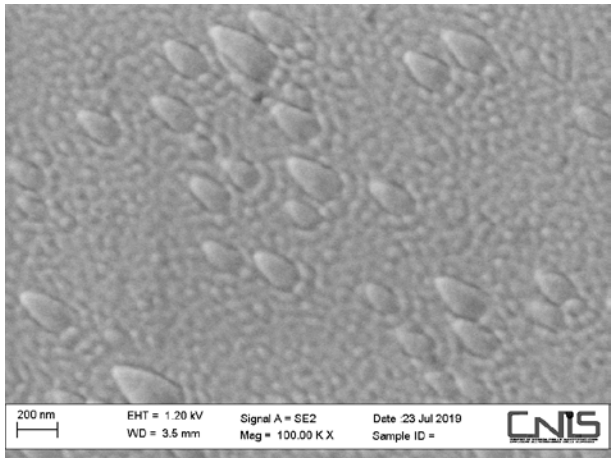

HA Cu 0 M_01